

Power Efficient Discontinuous Reception in THz and mmWave Wireless Systems

Syed Hashim Ali Shah, Sundar Aditya, Sourjya Dutta, Christopher Slezak and Sundeep Rangan
NYU WIRELESS, Tandon School of Engineering, New York University, Brooklyn, NY 11201

e-mail: {s.hashim, sundar.aditya, sdutta, chris.slezak, srangan}@nyu.edu

Abstract—Discontinuous reception (DRX), where a user equipment (UE) temporarily disables its receiver, is a critical power saving feature in modern cellular systems. DRX is likely to be particularly aggressively used in the mmWave and THz frequencies due to the high front end power consumption. A key challenge of DRX in these frequencies is that individual links are directional and highly susceptible to blockage. MmWave and THz UEs will therefore likely need to monitor multiple cells in multiple directions to ensure continuous reliable connectivity. This work proposes a novel, heuristic algorithm to dynamically select the cells to monitor to attempt to optimally trade-off link reliability and power consumption. The paper provides preliminary estimates of connected mode DRX mode consumption using detailed and realistic statistical models of blockers at both 28 and 140 GHz. It is found that although blockage dynamics are faster at 140 GHz, reliable connectivity at low power can be maintained with sufficient macro-diversity and link prediction.

Index Terms—Discontinuous reception (DRX), terahertz (THz) communications, millimeter wave (mmWave) communications

I. INTRODUCTION

Mobile wireless communication in the mmWave and THz bands enables multi-Gbps peak throughput, but at the cost of high power consumption in both radio frequency front-end (RFFE) and digital baseband processor. As we will see below, peak power consumption in the UE in the THz frequencies can exceed 1 Watt, a large portion of the total smartphone power budget. Discontinuous reception (DRX) modes [1], [2] where a mobile device or user equipment (UE) temporarily disables its receiver radio frequency front end (RFFE), can offer significant power savings in cases where the traffic is intermittent.

A key challenge in implementing DRX in the mmWave and THz frequencies is that links are highly susceptible to blockage by many common materials, as well as the human body or hand [3]. Thus, small changes in the environment or orientation of the handset can lead to rapid drops in link quality [4]–[6]. Hence, in DRX mode, the UE will likely need to monitor multiple cells to maintain reliable connectivity. Indeed, macro-diversity has been long identified as key in mmWave cellular systems [7]. However, from an energy standpoint, monitoring multiple links reduces the inactive time, thus creating a trade-off of power consumption and reliability.

As communications move from the mmWave to the sub-THz bands, the channel dynamics will likely become much faster. For example, Fig. 1 shows the predicted fade with a human blocker following the 3GPP double knife-edge diffraction model [8]. We see that at 140 GHz, the blockage is both

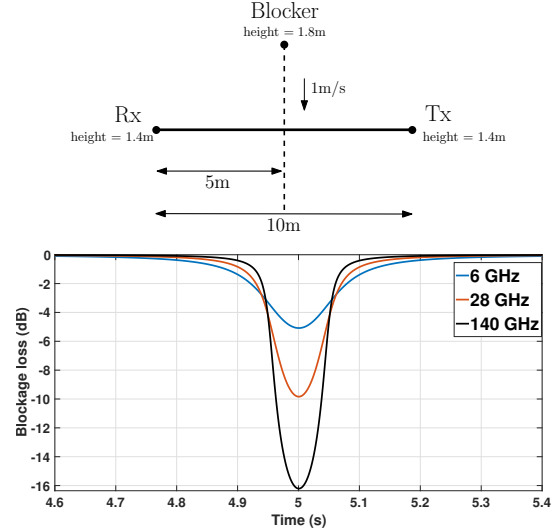


Fig. 1: Understanding the severity of blockages at higher frequencies. Top panel: Movement of a human blocker following the 3GPP model [8]. Bottom: Blockage loss due to knife-edge diffraction.

deeper and faster than 28 GHz. Faster channel dynamics will be harder to track and necessitate monitoring more cells for a given reliability. In addition, with the larger number of antenna elements and wider bandwidths, the RFFE power consumption will be higher. Hence, finding power efficient methods for properly selecting cells to monitor in DRX mode, will be even more vital.

The contribution of this paper is threefold. First, we provide a preliminary estimate of the power consumption per unit time for DRX mode measurements. We provide estimates at both 28 and 140 GHz. Second, to minimize the measurement wake time, we propose a simple algorithm where the UE tries to maintain its association to its current serving BS, while also tracking a subset (of a given cardinality) of the remaining BSs to mitigate the effects of blockage effects and also save power. Third, we provide detailed simulations of the algorithm using 3GPP path loss and blockage models [8].

II. FRONT END POWER CONSUMPTION AT THZ

We first attempt to estimate the power consumption for link monitoring in both mmWave and THz frequencies. For ultra-wideband systems, receivers (RXs) should be designed such that they can be programmed to tune into any assigned channel within the available frequency band. One such architecture is

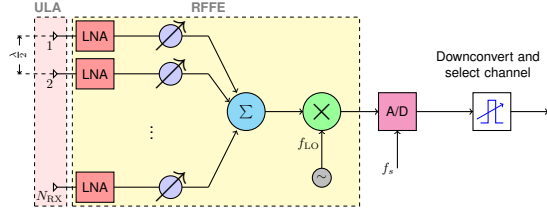


Fig. 2: Analog beamforming based multi-channel receiver front end with channel selection performed in digital base band.

proposed in [9], where down conversion and channel selection are performed by the baseband digital circuit. We will focus on *analog beamforming* as shown in Fig. 2, although similar calculations can be done for digital beamforming as well. For multi-channel operation, we assume the RFFE and the ADCs operate over the entire band.

ADC: The power consumed by an ADC scales linearly with the sampling frequency (f_s). For mmWave communications, 2 GHz of bandwidth is allocated around the center frequency of 28 GHz. Hence, ADCs for mmWave RFFE need to operate at $f_s = 2$ GHz. In contrast, 7 GHz of unlicensed spectrum is available in the THz band between 141 and 148 GHz [10]. Note that for the direct conversion architecture considered here, the ADCs operate over the entire available bandwidth although the individual component carriers may have a smaller bandwidths. This leads to a $3.5\times$ increase in power consumption, assuming that ADCs with the same figures of merit (FoMs) and resolution are used at both bands. In Table I, we consider an ADC FoM of 65 fJ/steps and we report the power consumed by a pair of 8-bit ADCs operating at $f_s = 2$ and $f_s = 7$ Gs/s at the Rx.

RFFE: For a given distance, the free space path loss encountered at 140 GHz is nearly 14 dB higher compared to 28 GHz mmWave bands. To mitigate this loss in link budget through beamforming, THz transmitters and receivers will require at least a quadrupling of the number of antenna elements on both sides of the link. However, due to the decreased wavelength, the total antenna aperture can be decreased or even reduced if there is gain increase on both sides. For example, a 4×4 uniform plane array (UPA) with $\lambda/2$ spacing at 28 GHz would require approximately an 2×2 cm² area, while an 8×8 array at 140 GHz would require approximately an 0.8×0.8 cm² area.

An increase in the number of antennas for an analog beamformer implies an increase in the number of low noise amplifiers (LNAs) and RF phase shifters (PSs). Following the work in [11], we assume that the PSs, combiners and mixers are passive circuits. We also make the assumption that the FoM for the LNAs and the insertion loss (IL) due to the PSs and mixers are the same as at 28 GHz [11] and 140 GHz. In Table I, we compare the power drawn by the RFFE of a Rx at 28 GHz with 8-antennas and one at 140 GHz with 64 antennas assuming a 10 dBm of local oscillator power draw.

One might argue that the RFFE power draw may be reduced by sophistication in circuit design that enhances the

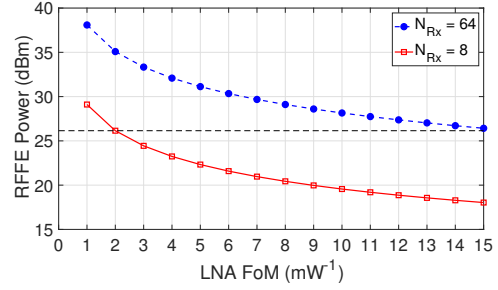


Fig. 3: RFFE power consumption as a function of the LNA FoM. For mathematical expressions see [11]

Component	28 GHz ($N_{rx} = 8$)	140 GHz ($N_{rx} = 64$)
RFFE	133.7	999.3
ADC	66.6	232.9
Total	200.3	1232.2

TABLE I: Power consumption by Rx front end at mmWave and THz (all units in mW)

performance of the LNAs and the PSs. But this may not be the case. As shown in Fig. 3, a 64 element system with a very high LNA FoM of 15 mW^{-1} draws the same power as an 8 element system with a low LNA FoM of 2 mW^{-1} . Similar observations can be made about PS IL as well. In fact, even with considerable advancements in devices and circuit design, a 64 element RFFE will draw considerably more power than a 8 element one.

Due to the use of a large number of antennas and very wideband data converters, cellular front ends at 140 GHz can consume nearly a Watt of additional power compared to those at 28 GHz as evident from Table I. Hence, power saving at the receiver by optimizing the discontinuous reception (DRX) procedure can be crucial for such systems, especially when employed in handheld UEs.

III. SYSTEM MODEL

DRX is used at the UE both in the RRC connected mode (i.e., between active data transmissions) as well as the RRC idle and RRC inactive modes (i.e., when there is a long period of inactivity) [12]. In this work, we focus on the connected mode DRX, which is key for UE power savings especially under practical bursty traffic considerations and multi-user scenarios. To support macro-diversity resistance against blockage, we assume the network maintains multiple simultaneous connections to the UE from different cells (e.g. via carrier aggregation). The set of cells from which data can be transmitted is called the *serving set*.

During DRX, the UE turns off its Rx FE and goes into the “sleep mode” to save power. Periodically, the UE “wakes up” at pre-allocated time instances to either monitor a subset of the available links, or transmit and receive control signals. During the monitoring intervals, the UE measures the links over an interval of duration T_{SS} as shown in Fig. 4. We assume the UE will measure link quality from the synchronization

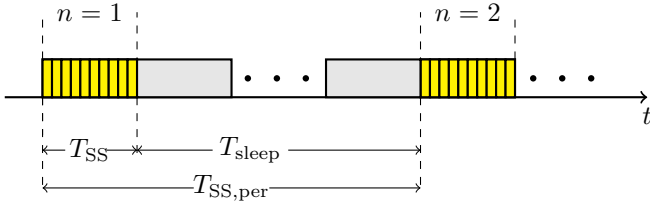


Fig. 4: Time line of a UE in connected mode DRX.

signal bursts (SSBs) transmitted by the tracked BS. The typical periodicity for the SSBs is $T_{SS,per} = 20$ ms [13], [14].

We assume each BS has a different pointing angle to the UE. Therefore the number of scans the UE needs to perform increase with the number of cells to monitor. To save power, we assume that the UE can monitor a subset of the serving cells, which we call the *listening set*. Hence, the value of T_{SS} will be determined by the number of cells in the listening set, and the UE will be in sleep mode for a duration $T_{sleep} = T_{SS,per} - T_{SS}$ in each DRX cycle.

Blockage: Our goal is to quantify the trade-off of monitor power consumption and blockage. To model the blockage, let M_u and M_b denote the number of antenna elements at the UE and each cell or BS, respectively. Within the DRX cycle, we index the monitoring or “awake” periods by $n = 1, 2, \dots$ as shown in Fig. 4. We term them as “monitoring instances”. Let $\mathbf{H}^{(n,k)} \in \mathbb{C}^{M_u \times M_b}$ denote the channel matrix between the UE and the k -th cell in the n -th monitoring instance. The signal received at the UE is given by

$$y_{nk} = \mathbf{w}_k^H \mathbf{H}^{(n,k)} \mathbf{f}_k x + \xi_{nk}, \quad (1)$$

where $\mathbf{w}_k \in \mathbb{C}^{M_u \times 1}$ and $\mathbf{f}_k \in \mathbb{C}^{M_b \times 1}$ are the beamforming vectors applied at the UE and the cell, respectively, for the given link, x is the unit energy measurement signal, and $\xi_{nk} \sim \mathcal{CN}(0, \sigma^2)$ is the system noise. Hence, for the measurement signal transmitted from the k -th cell, the signal-to-noise ratio (SNR) at the UE is

$$\gamma_{nk} = \frac{|\mathbf{w}_k^H \mathbf{H}^{(n,k)} \mathbf{f}_k|^2}{\sigma^2}. \quad (2)$$

Let $\mathcal{A}_n \subseteq \{1, \dots, N\}$ denote the listening set, which is the set of cells chosen in the n -th monitoring instance. We refer to \mathcal{A}_n as the *listening set*. We let K denote the number of cells in the listening set. Listening to fewer cells during each monitoring instance implies that the Rx FE is turned on for a short period of time, which saves power. However, with small K , it is more probable that all the links in \mathcal{A}_n are blocked. For a given listening set, the probability of blocking, denoted by P_B , can be expressed as follows:

$$P_B \approx \prod_{k \in \mathcal{A}_n} \mathbb{P}(\gamma_{nk} < \gamma_{\min}), \quad (3)$$

where γ_{\min} is the minimum SNR required for signal detection or decoding. This leads to an interesting trade-off. Listening to a large number of cells ensures that the UE has a higher probability of having a usable radio link. But this will require

larger wake periods during the DRX cycle, leading to greater power draw.

We use the following simple model to quantify the trade-off. We assume that the time to monitor K cells is $T_{SS} = KT_{SS,0}$, where $T_{SS,0}$ is the time to monitor each cell. If at least one link in the monitoring interval is not blocked, the UE will spend a fraction $KT_{SS,0}/T_{SS,per}$ of the DRX cycle monitoring the link. If all links are blocked, we assume that the UE must stay awake for at least one entire DRX cycle to perform a complete beam search, and re-establish a reliable connection. Under the above model, the fraction of time the UE is awake, β_{awake} , and the corresponding time the UE is asleep β_{sleep} can be bounded as,

$$\beta_{\text{awake}} \geq (1 - P_B) \frac{KT_{SS,0}}{T_{SS,per}} + P_B, \quad (4)$$

$$\beta_{\text{sleep}} = 1 - \beta_{\text{awake}}, \quad (5)$$

where the inequality in (4) results from the fact that the UE might have to be awake for more than $T_{SS,per}$ on link failure. Equations (4)-(5) shows the trade-off between the listening set size and power savings in the DRX cycle. This is studied through cellular simulations both at 28 and 140 GHz in the following section.

IV. DRX MEASUREMENTS AND POWER SAVINGS

To address the problem of saving power by optimizing the DRX cycle under blockage limited access, in this section we propose a simple algorithm. In Algorithm 1, for a given K , the UE selects the best K cells out of all the N cells before going into DRX mode, i.e., at time $n = 0$. Before going into the DRX cycle, based on the N measurements, the UE selects

Algorithm 1 Proposed Algorithm

Data: $\{\gamma_{nk} : k = 1, \dots, N; n = 1, 2, \dots\}$

Input : K, γ_{\min}

Initialization

- Listen to all cells and choose the one with the highest SNR as the serving cell.
- Choosing listening set \mathcal{A}_n : In addition to the serving cell, uniformly select a subset of $K - 1$ cells from the remaining $N - 1$ cells.

Operation ($n \geq 1$)

- Measure γ_{nk} for $k \in \mathcal{A}_n$. Let $\gamma_{n,0}$ denote the SNR of the serving cell.
 - if** $\gamma_{n,0} > \gamma_{\min}$ **then**
 - $\gamma_{n+1,0} = \gamma_{n,0} \rightarrow$ *Stick to current BS*
 - else**
 - if** $\max_{k \in \mathcal{A}_n} \gamma_{nk} > \gamma_{\min}$ **then**
 - $\gamma_{n+1,0} = \max_{k \in \mathcal{A}_n} \gamma_{nk} \rightarrow$ *Change serving cell*
 - else**
 - Trigger exhaustive beam sweep: Go back to initialization*
 - end**
-

K BS (the listening set \mathcal{A}_n) to monitor during the DRX cycle including the primary associated link. In the DRX cycle the link quality of all the BSs in \mathcal{A}_n are measured.

Let the SNR of the serving BS at the n -th measurement period be $\gamma_{n,0}$. If $\gamma_{n,0} \geq \gamma_{\min}$, the UE does not change the serving BS. Otherwise, if $\gamma_{n,0} < \gamma_{\min}$, the UE changes its serving BS and chooses the best BS in \mathcal{A}_n such that

$$\gamma_{n+1,0} = \max_{k \in \mathcal{A}_n} \gamma_{nk}. \quad (6)$$

Since the UE will already have synchronization information from the BSs contained in \mathcal{A}_n , it will only need to do a random access to change the serving BS. However, when all the links in \mathcal{A}_n are blocked, i.e.,

$$\max_{k \in \mathcal{A}_n} \gamma_{nk} < \gamma_{\min}, \quad (7)$$

the UE has to go through the beam sweep procedure. The beam sweep procedure for beamformed systems can span over several SS periods. The time taken by beam sweep can hence be given as $T_{\text{BSW}} = L \times T_{\text{SS,per}}$, where $L \geq 1$. The algorithm is summarized in Algorithm 1.

V. NUMERICAL RESULTS

A. Simulation Setup

We generate 100 channel trajectories at 28 GHz and 140 GHz using end-to-end simulations that are mainly based on the 3GPP channel model in [8]¹. The UE is located at (0, 0, 1.8) m. At 28 GHz, we consider 8 antenna elements at the UE, while at 140 GHz, 64 antenna elements are assumed. For simplicity, we do not consider the impact of array geometry and the associated latency and the power consumption involved in finding the best receive direction. Instead, we assume eigen beamforming to calculate the beamforming gain in (2) (i.e., \mathbf{w}_k and \mathbf{f}_k are equal to the eigenvector corresponding to the largest eigenvalue of $\mathbf{H}^{(n,k)} \mathbf{H}^{(n,k)H}$ and $\mathbf{H}^{(n,k)H} \mathbf{H}^{(n,k)}$, respectively). Hence, in effect, we assume that the UE and the BS can always ‘point’ towards each other and determine the strongest direction of the received signal. The challenges posed by array geometry is left for future work.

We consider a cell radius, (r), of 100 m and deploy 9 BSs of height 10m in the xy -plane on a square grid of dimensions 200 m \times 200 m. The BSs can either be in line-of-sight or non-line-of-sight. At 28 GHz and 140 GHz, we consider the number of antennas at the BS to be 64 and 256 respectively. The UE is dropped randomly within the grid for a given channel trajectory and remains stationary.

We distinguish between two kinds of blockers - human and vehicular, which are assumed to be present with equal probability. The blockage loss is modeled using the 3GPP blockage model B [8], which is based on double knife-edge diffraction, where each blocker is modeled as rectangular screen in the vertical plane. The blocker dimensions are chosen according to 3GPP recommendations [8], with the height and

width of a human (vehicular) blocker set to 1.7 m (1.4 m) and 0.3 m (4.8 m), respectively. For a given channel trajectory, let $\mathbf{x}_j(n) \in \mathbb{R}^2$ denote the projection of the centroid of the j -th blocker onto the xy -plane during the n -th monitoring instance. At $n = 0$, the collection of obstacle locations, $\{\mathbf{x}_j(0)\}$, are distributed according to a Poisson point process of intensity $\lambda_b = 0.01 \text{ m}^{-2}$ [15] over a circle of radius 200 m centered at the UE. For $n \geq 1$, $\mathbf{x}_j(n)$ evolves in a Markovian manner as follows:

$$\mathbf{x}_j(n) = \mathbf{x}_j(n-1) + \dot{\mathbf{x}}_j(n)\Delta, \quad (8)$$

where $\dot{\mathbf{x}}_j(n) \in \mathbb{R}^2$ denotes the velocity along the xy -plane of the j -th obstacle during the n -th monitoring instance and $\Delta = 20 \text{ ms}$ is the sampling period (SSB periodicity [13], [14]).

The initial blocker velocities, $\{\dot{\mathbf{x}}_j(0)\}$, are drawn independently and uniformly over $[0, 1] \text{ m/s}$ for a human blocker and over $[0, 28] \text{ m/s}$ for vehicular blockers². For $n \geq 1$, $\dot{\mathbf{x}}_j(n)$ evolves in the following manner:

$$\dot{\mathbf{x}}_j(n) = \dot{\mathbf{x}}_j(n-1) + \mathbf{w}(n) \quad (9)$$

where $\{\mathbf{w}(n) : n \geq 1\}$ is a sequence of i.i.d zero-mean Gaussian random vectors with identity covariance matrix. For simplicity, we assume \mathbf{w}_k and \mathbf{f}_k to be equal to the left and right singular vectors corresponding to the largest singular value of $\mathbf{H}^{(n,k)}$, respectively.

The list of all the parameters used for generating the channel trajectories are provided in Table II.

B. Simulation Results

The performance of Algorithm 1 is evaluated using the SNR from the generated channel trajectories. The quantities of interest, as a function of K , are the blocking probability, P_B ($\gamma_{\min} = -6.5 \text{ dB}$) and the fractional UE sleeping time, β_{sleep} .

²These velocity ranges for human and vehicular blockers are based on 3GPP recommendations, as well [8].

Parameters	28 GHz	140 GHz
Scenario	UMi	
M_u	8	64
M_b	64	256
BS height	10 m	
N	9	
UE height	1.8m	
Bandwidth	400 MHz	
Sampling interval	20 ms	
Temperature	298 K	
Cell radius, r	100 m	
Blocker density, λ_b	0.01 m^{-2}	
Blocker height	1.4 m (Vehicular), 1.7 m (Human)	
Blocker width	4.8 m (Vehicular), 0.3 m (Human)	
Blocker speed	0-28 m/s (0-100 km/h)[Vehicular] 0-1 m/s (0-3 km/h)[Human]	
Transmitted Power	23dBm	

TABLE II: Values of different parameters for the generation of channel trajectories

¹While the specifications of the 3GPP channel model are valid up to 100GHz, we continue to use it even for 140GHz due to the absence of standardized channel models for the spectrum above 100 GHz

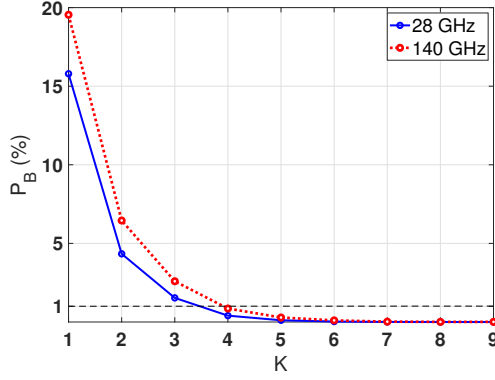


Fig. 5: Variation of P_B as a function of K . The dashed horizontal line corresponds to $P_B = 1\%$.

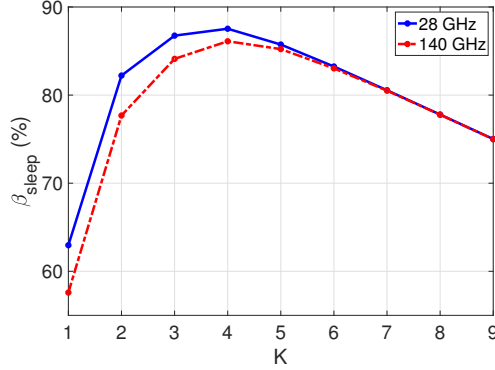


Fig. 6: Fractional UE sleep time, β_{sleep} , as a function of K .

Fig. 5 captures the variation in P_B as a function of K . We observe that $K = 4$ is sufficient to guarantee a usable radio link with a probability greater than 99%.

Fig. 6 plots β_{sleep} as a function of K . While it seems intuitive to expect that β_{sleep} would be the highest for $K = 1$, since T_{SS} has the smallest value in this case, this is not true in reality since the probability that the UE has to perform exhaustive beam sweep (equal to P_B) is also high. At the other extreme when $K = 9$, even though the UE does not have to perform beam sweep often, β_{sleep} is still not the highest due to the large value of T_{SS} . From Fig. 6, we observe that β_{sleep} is highest ($> 85\%$ for 28 GHz and 140 GHz) when $K = 4$. Thus, from Figs. 5 and 6, we infer that $K = 4$ is sufficient to guarantee a usable radio link at least 99% of the time while saving the most amount of power.

VI. CONCLUSION

A central challenge for realizing mobile and handheld devices in the mmWave and THz frequencies is the high power consumption of the RFFE. Aggressive use of DRX modes offers the possibility of significant power savings, assuming traffic is bursty. However, mmWave and THz channel quality can be intermittent due to blockage. frequent channel monitoring in DRX mode thereby reducing the power savings. In this work, we have presented preliminary estimates of

RFFE power consumption for DRX measurements. A simple algorithm to minimize the number of cells to monitor has also been proposed and simulated at both 28 and 140 GHz. Our simulations indicate that, using correct predictions, a small number of cells can be tracked, while maintaining high levels of reliability.

ACKNOWLEDGEMENTS

This work was supported by the National Science Foundation under Grants 1302336, 1564142, and 1547332, NIST, SRC and the industrial affiliates of NYU WIRELESS.

REFERENCES

- [1] J. Zhou, N. Nikaein, and T. Spyropoulos, "LTE/LTE-A discontinuous reception modeling for machine type communications," *IEEE Wireless Commun. Lett.*, vol. 2, no. 1, pp. 102-105, 2013.
- [2] H. Ramazanali, "Performance evaluation of LTE/LTE-a DRX: A Markovian approach," *IEEE Internet Things J.*, vol. 3, no. 3, pp. 386-397, 2016.
- [3] T. S. Rappaport, R. W. Heath Jr, R. C. Daniels, and J. N. Murdock, *Millimeter wave wireless communications*. Pearson Education, 2014.
- [4] C. Slezak, V. Semkin, S. Andreev, Y. Koucheryavy, and S. Rangan, "Empirical effects of dynamic human-body blockage in 60 GHz communications," *IEEE Commun. Mag.*, vol. 56, no. 12, pp. 60-66, 2018.
- [5] V. Raghavan, V. Podshivalov, J. Hulten, M. A. Tassoudji, A. Sampath, O. H. Koymen, and J. Li, "Spatio-temporal impact of hand and body blockage for millimeter-wave user equipment design at 28 GHz," *IEEE Commun. Mag.*, vol. 56, no. 12, pp. 46-52, 2018.
- [6] G. R. MacCartney, T. S. Rappaport, and S. Rangan, "Rapid fading due to human blockage in pedestrian crowds at 5g millimeter-wave frequencies," in *Proc. IEEE GLOBECOM*, 2017, pp. 1-7.
- [7] J. Choi, "On the macro diversity with multiple bss to mitigate blockage in millimeter-wave communications," *IEEE Commun. Lett.*, vol. 18, no. 9, pp. 1653-1656, 2014.
- [8] 3GPP, "TR 38.901, study on channel model for frequencies from 0.5 to 100 GHz (release 15) document," Jun. 2018.
- [9] S. Hwu and B. Razavi, "An RF receiver for intra-band carrier aggregation," *IEEE J. Solid-State Circuits*, vol. 50, no. 4, pp. 946-961, Apr. 2015.
- [10] "FCC online table of frequency allocations," Federal Communications Commission, Tech. Rep. 47 C.F.R. 2.106, 2018. [Online]. Available: <https://transition.fcc.gov/oet/spectrum/table/fcctable.pdf>
- [11] S. Dutta, C. Barati, A. Dhananjay, D. A. Ramirez, J. F. Buckwalter, and S. Rangan, "A case for digital beamforming at mmWave," *arXiv preprint arXiv:1901.08693*, 2019.
- [12] 3GPP, "TS 38.300, NR and NG-RAN Overall Description; Stage 2," 2017.
- [13] —, "TS 38.331 NR - Radio Resource Control (RRC) protocol specification - Release 15," 2017.
- [14] M. Giordani, M. Polese, A. Roy, D. Castor, and M. Zorzi, "A tutorial on beam management for 3gpp nr at mmwave frequencies," *arXiv preprint arXiv:1804.01908*, 2018.
- [15] I. K. Jain, R. Kumar, and S. Panwar, "Limited by capacity or blockage? a millimeter wave blockage analysis," *Proc. Intl. Teletraffic Congress*, pp. 153-159, 2018.